Adiabatic Spin Pumping with Quantum Dots

Eduardo R. Mucciolo

Department of Physics, University of Central Florida, P.O. Box 162385, Orlando, FL 32816-2385, USA

Summary. Electronic transport in mesoscopic systems has been intensively studied for more the last three decades. While there is a substantial understanding of the stationary regime, much less is know about phase-coherent nonequilibrium transport when pulses or ac perturbations are used to drive electrons at low temperatures and at small length scales. However, about twenty years ago Thouless proposed to drive nondissipative currents in quantum systems by applying simultaneously two phase-locked external perturbations. The so-called adiabatic pumping mechanism has been revived in the last few years, both theoretically and experimentally, in part because of the development of lateral semiconductor quantum dots. Here we will explain how open dots can be used to create spin-polarized currents with little or no net charge transfer. The pure spin pump we propose is the analog of a charge battery in conventional electronics and may provide a needed circuit element for spin-based electronics. We will also discuss other relevant issues such as rectification and decoherence and point out possible extensions of the mechanism to closed dots.

1 Introduction

In the past few years we have seen important advances in the coherent control of micro and nanoelectronic devices. The experimental effort, driven by the quest for the implementation of quantum computation in semiconductor and superconductor devices, has increased substantially the breath and scope of the study of mesoscopic systems, in particular lateral semiconductor quantum dots [1]. In these systems, electrons within a two-dimensional gas (2DEG) are confined to small puddles by the application of gate voltages. The shape and size of these puddles can be controlled and fine tuned by the same or additional gate voltages. Electrodes also allow one to vary the width of the point contacts that connect the electron puddle to the 2DEG. By acting on these points contacts one can operate the quantum dots in "open" (at least

one propagating channel allowed per point contact) or "closed" (fully pinched point contacts) regimes.

A great variety of *stationary* transport phenomena has been observed in these systems over the past fifteen years, from discrete Coulomb blockade [1] to signatures of chaotic orbits [2, 3, 4] and the Kondo effect [5, 6]. Recently, a new generation of experiments has started to probe the *dynamical* transport properties of quantum dots. A remarkable attempt to explore phase-coherent, pulsed response of an open quantum dot was led by Stwikes and collaborators [7]. Their motivation was the observation of the so-called *adiabatic quantum pumping effect*, first discussed by Thouless in the context of one-dimensional electronic systems more than twenty years ago [8]. Adiabatic quantum pumping takes place when one slowly modulates two or more external parameters of a quantum system, resulting in a net dc current without the application of any bias [9, 10, 11, 12, 13]. The effect requires phase-coherent electrons and a system well coupled to reservoirs. Since the original proposal by Thouless appeared, quantum pumping has been explained, reinterpreted, discussed, and extended by many authors, to the point that a complete and fair review of the literature would take a large portion of this book. Here, we will only refer to those works which are of significance to the main subject of this lecture.

The generation of spin currents in semiconductor heterostructures is a topic of great interest presently [14, 15]. It is believed that spin currents may find applications in in-chip quantum communication, where light propagation is not practical. The full control of the electronic spin degree of freedom in semiconductors also promises to have a large impact in the future of conventional technologies by increasing processing speed, storage capacity, and functionality. While our work does not explore these issues, it does show that quantum dots are versatile enough to yield spin currents with high efficiency, albeit only at low temperatures.

The remaining sections are divided as follows. In Sec. 2 we provide a general discussion of adiabatic quantum pumping based on the scattering matrix formalism. In Sec. 3 we show that pumping in the presence of a sufficiently strong magnetic breaks spin symmetry and produces spin-polarized currents. We also estimate the magnitude of the effect under realistic assumptions. The detection of pure spin currents generated with a quantum dot spin pump is discussed in Sec. 4, together with the importance of spurious rectification effects and dephasing. Finally, in Sec. 5 we point out unexplored aspects of quantum pumping and some promising future directions.

2 Adiabatic Quantum Pumping

Let us suppose that a certain quantum system is connected to two or more particle reservoirs. Quantum pumping can be defined as the production of net dc currents between reservoirs by acting solely on the quantum system with ac perturbations. No bias is applied between reservoirs. For open quantum

systems, when no substantial potential barriers exist between the system and the reservoirs, adiabatic pumping is achieved when the frequency of the ac perturbations is much smaller than the inverse particle dwell time, $\omega \ll 1/\tau_{\rm d}$. ($\tau_{\rm d}$ is defined as the typical time a particle spends inside the quantum system.) For adiabatic pumping one needs to vary at least two independent parameters, say, X_1 and X_2, to induce a dc current. In Fig. 1 we show schematically how a quantum pump can be implemented with a lateral quantum dot.

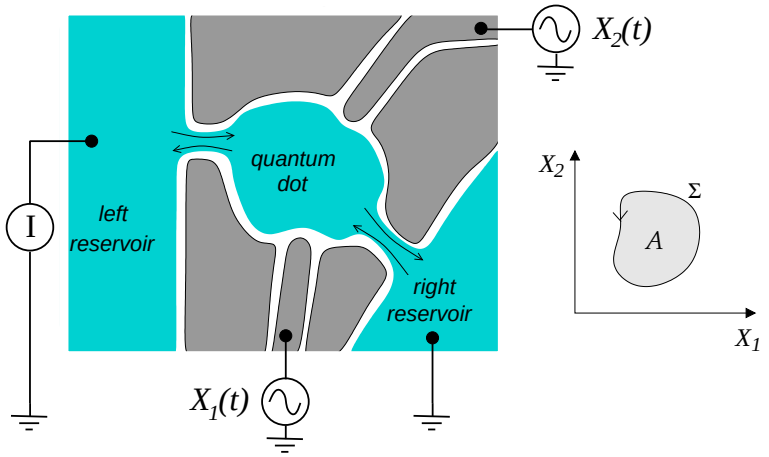

Fig. 1. A quantum dot electron pump. The dark gray elements represent electrodes and the arrows indicate electron flow through the dot-reservoir contact regions. The two gate voltages $X_1(t)$ and $X_2(t)$ act as pumping parameters, continuously deforming the dot shape. On the right-had side: a pumping cycle in parameter space. The voltages sweep a closed area $\mathcal{A}$ with contour Σ in parameter space. After a cycle is completed, a net charge is transfered between the two reservoirs

2.1 Scattering Matrix Formulation

There is a simple and elegant way to formulate quantum pumping in the language of scattering matrices [11]. Let us define δq_α as the amount of charge that passes through the channel α in one of the contacts during a time interval δt. During this interval, the external parameters X_1 and X_2 vary by $\delta X_1 = \dot{X}_1\, dt$ and $\delta X_2 = \dot{X}_2\, dt$, respectively. Assuming that δX_1 and δX_2 are small, we can use linear response theory and write

$$\delta q_\alpha(t) = e\left[A_{\alpha;1}\,\dot{X}_1(t) + A_{\alpha;2}\,\dot{X}_2(t)\right]\,\delta t, \tag{1}$$

where e is the electron charge and the quantities $A_{\alpha;1,2}$ are called emissitivites. The emissivities depend implicitly on time through $X_1(t)$ and $X_2(t)$. They

can be written in terms of the scattering matrix of the quantum system (see below). Notice that (1) assumes that the response is instantaneous (local in time). This is correct provided that we are in the weak perturbation, adiabatic regime: $|\dot{X}_j| \ll |X_j|/\tau_{\rm d}$ for $j = 1, 2$. If we now want to calculate the net charge that flowed through channel α after a full pumping cycle is completed (namely, after a period equals to $2\pi/\omega$), we have that

$$q_\alpha = \int_{\rm cycle} \delta q_\alpha(t) = e \int_0^{2\pi/\omega} dt \, \left(\dot{X}_1 \, A_{\alpha;1} + \dot{X}_2 \, A_{\alpha;2} \right). \tag{2}$$

We can use Green's theorem to convert the integral over time into an area integral in parameter space. The result is

$$q_\alpha = e \int_{\mathcal{A}} dX_1 dX_2 \, \left(\frac{\partial A_{\alpha;2}}{\partial X_1} - \frac{\partial A_{\alpha;1}}{\partial X_2} \right). \tag{3}$$

Notice the similarity between (3) and the expression defining a magnetic flux through a loop of area $\mathcal{A}$. Here, the integrand plays the role of a fictitious magnetic field pointing perpendicularly to the $X_1 - X_2$ plane and whose vector potential has in-plane components $A_{\alpha;1}$ and $A_{\alpha;2}$.

The connection to the quantum system scattering matrix $\hat{S}$ occurs through the following expression, first derived by Büttiker and collaborators [16]:

$$A_{\alpha;j} = \frac{1}{2\pi} {\rm Im} \left[\frac{\partial \hat{S}}{\partial X_j} \hat{S}^\dagger \right]_{\alpha\alpha}. \tag{4}$$

It is then straightforward to derive the following expression for the total charge pumped through channel α [11]:

$$q_\alpha = \frac{e}{\pi} \int_{\mathcal{A}} dX_1 dX_2 \, {\rm Im} \left[\frac{\partial S}{\partial X_2} \frac{\partial S^\dagger}{\partial X_1} \right]_{\alpha\alpha}, \tag{5}$$

There are several alternative ways to arrive at (5). We would like to refer in particular to the insightful derivation presented by Avron and collaborators in Ref. [17], who also give an interesting physical interpretation of (4). The large sensitivity of the scattering matrix elements to interference inside the quantum dot makes the pumped charge is a strongly fluctuating quantity.

At this point, the message is that knowing how the quantum dot scattering matrix depends on the external parameters X_1 and X_2 allows one to compute the pumping current in the adiabatic regime. However, there are a few subtle aspects that have been omitted in this discussion. First is the assumption that particles keep their energy as they go in and out of the quantum dot, namely, that the adiabatic process is elastic. This is not exactly true since the system+reservoir Hamiltonian is time-dependent. However, it should be a reasonable approximation in the adiabatic regime, when incoming and outgoing particles see the quantum dot essentially as a nearly static scatterer. Thus, the pumped charge in (5) depends on a single, fixed particle energy.

Second, since the reservoirs are Fermi seas, the particles participating in the transport will have their energies distributed over a continuum at finite temperatures. To account for that, we integrate $q_\alpha = q_\alpha(E)$ over energy, appropriately weighted by the derivative of the Fermi distribution,

$$\begin{aligned} Q_\alpha &= \int_0^\infty d\varepsilon \left(-\frac{\partial f}{\partial \varepsilon}\right) q_\alpha(\varepsilon) \\ &= \frac{e}{\pi} \int_0^\infty d\varepsilon \left(-\frac{\partial f}{\partial \varepsilon}\right) \int_{\mathcal{A}} dX_1 dX_2 \,\mathrm{Im}\left[\frac{\partial S}{\partial X_2}\,\frac{\partial S^\dagger}{\partial X_1}\right]_{\alpha\alpha}, \end{aligned} \tag{6}$$

with $f(\varepsilon) = 1/[\exp(\varepsilon-\mu)/k_BT+1]$. Above, it is implicitly understood that $S = S(\varepsilon, X_1, X_2)$ and that the two reservoirs have the same equilibrium properties, namely temperature T and chemical potential μ (i.e., no bias is applied). It is clear that (6) is reduced to (5) evaluated at the Fermi energy as $T \to 0$.

At this point it is worthwhile deriving an expression for the dc component of the pumping current in some simple situation. For instance, let us assume that the pumping parameters vary as $X_1(t) = X_{01} + \delta X_1 \cos(\omega t)$ and $X_2(t) = X_{02} + \delta X_2 \cos(\omega t - \varphi)$, with amplitudes δX_1 and δX_2 so small that the integrand in (6) is essentially constant over the pumping cycle. It is not difficult to show that, in this case,

$$I_\alpha = \frac{\omega\, Q_\alpha}{2\pi} \approx e\,\omega\,\sin\varphi\;\delta X_1 \delta X_2\, \mathcal{I}_\alpha, \tag{7}$$

where

$$\mathcal{I}_\alpha = \frac{1}{\pi} \int_0^\infty d\varepsilon \left(-\frac{\partial f}{\partial \varepsilon}\right) \mathrm{Im}\left[\frac{\partial S}{\partial X_2}\,\frac{\partial S^\dagger}{\partial X_1}\right]_{\alpha\alpha} \tag{8}$$

In this regime, the pumping current is a bilinear function of the pumping amplitudes and has a sinusoidal dependence on the phase difference ϕ.

The small-amplitude approximation ceases to be valid when $|X_i| \gg X_i^{(c)}$, $i = 1, 2$, where $X_1^{(c)}$ and $X_1^{(c)}$ are the characteristic parameter scales over which the scattering matrix elements change substantially. For large parameter amplitudes, the integrand in (6) will fluctuate and change sign many times within the integration area A. As a result, the pumping charge will depend on the parameter amplitudes as $\sqrt{\delta X_1\, \delta X_2}$ rather than bilinearly [11]. Moreover, one expects to observe a more complicated dependence on ϕ.

Most of these features were observed in a experiment by Switkes and coworkers using an open lateral quantum dot subjected to two ac, shape deforming gate voltages [7]. In that experiment, the electron dwell time in the quantum dot was estimated to be under 1 ns, while the pumping frequency used was in the tens of MHz. Therefore, the pumping regime was certainly adiabatic. However, a few aspects of the experimental data were in conflict with the theoretical predictions [11, 13]. The discrepancies involved the amplitude of the quantum pumping current and its symmetry properties in the presence of an external magnetic field. In the next section we briefly describe

the statistics and symmetry of pumping currents. As pointed out by Brouwer, that early experiment was likely plagued by spurious rectification effects due the capacitive coupling between gates and electron reservoirs [18].

2.2 Statistical and Symmetry Properties of Pumping Current

Phase coherence is at the heart of adiabatic quantum pumping. The pumping current amplitude is a very sensitive function of the spatial structure of the wave function inside the quantum dot. That structure in turn is a manifestation of electron interference and therefore very sensitive to changes in the shape of the confining potential. One expects that different realizations of the dot geometry will lead to marked changes in the amplitude and direction of the pumping current. A weak magnetic field that scrambles the electron phase with little effect on the orbital motion will also cause a similar effect. Such mesoscopic fluctuations were indeed observed in Ref. [7].

There is a vast literature treating the statistical properties of the scattering matrix in chaotic mesoscopic systems (see Ref. [19] for a review). Using this accumulated knowledge, it is possible to determine the full distribution of the pumping current for all relevant universal symmetry classes and for any number of propagating channels in the contacts [11]. At zero temperature, it was found that the distribution ranges from nearly Gaussian when the contacts carry many propagating channels ($N = N_R + N_L \gg 1$) to a singular form with power-law tails when $N_R = N_L = 1$ (one propagating channel per contact). For the single-channel case, $P(I) \sim 1/|I|^{\kappa}$ for large I, where $\kappa = 9/4$ (3) when time-reversal symmetry is present (absent). Thus, while the ensemble average of the pumping current is always zero at zero bias, $\langle I \rangle = 0$, the variance is always nonzero and actually diverges for the $N_R = N_L = 1$ case. In practice, these very large mesoscopic fluctuations are capped by the finite decoherence times of real systems [20, 21]. For $N > 2$, thermal fluctuations also decrease the amplitude of the pumping current.

The effect of discrete spatial symmetries and magnetic field inversion on the adiabatic quantum pumping current can also be understood through the scattering matrix formalism described in Sec. 2.1. After some initial controversy in the literature, this issue was lucidly discussed in Ref. [22]. The most important property to mention in regard to symmetry is the following: For open quantum dots with no discrete spatial symmetry, there is no particular symmetry in the pumping current with respect to the inversion of the magnetic field:

$$I(B) \neq I(-B) \qquad \text{for a completely asymmetric dot.} \tag{9}$$

In other words, there is no counterpart to the Onsager relation characteristic of biased dissipative transport. The experiment of Ref. [7] was not consistent with this prediction. This fact and others indicate that this early attempt to observe quantum pumping was likely dominated by rectification effects (which should yield $I(B) = I(-B)$).

Interestingly, it is also possible to show that for a pump with inversion symmetry (left-right and top-bottom symmetries), there is always a perfect cancellation of charge flow during the pumping cycle, yielding $I = 0$ identically.

3 Pumping Spin with Quantum Dots

The quantum pumping current described in Sec. 2 contained spin-degenerate electrons. Therefore, the contributions coming from "up" and "down" spin components of the charge current had identical direction and amplitude, leading to zero net spin or angular momentum transport. In order to generate a net spin flow out of spin-depolarized electron sources, one needs to add a spin-symmetry breaking field to the system. There are two simple ways to do that: (i) creating a Zeeman splitting in the spectrum by applying an external magnetic field, or (ii) using a pump with strong spin-orbit coupling. While the latter has been recently studied theoretically in different contexts [23, 24], it remains very challenging to implement experimentally. Here we will focus on the former case [25], which has already been tested and shown to produce clear evidence of spin-polarized transport [26].[1]

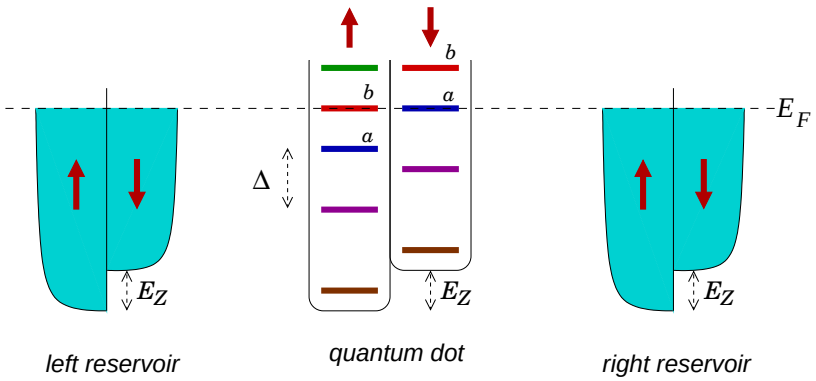

Fig. 2. Schematic view of the states involved in the quantum pumping current through a dot in the presence of a Zeeman energy splitting E_Z of the order of the mean level spacing Δ. The solid arrows indicate spin orientation. The Zeeman splitting does not significantly modify the nature of the states in the reservoirs found near the Fermi level. However, if a and b are states with distinct wave function content, the splitting can make $I_\uparrow \neq I_\downarrow$

The main idea can be understood through the scheme shown in Fig. 2. Since the materials underlying reservoirs and quantum dot is the same, upon

[1] Spin pumping in interacting nanowires was first discussed in Ref. [27] and further extended in Ref. [28].

the application of an external magnetic field B, energy levels inside and outside the dot will be spin split by the Zeeman energy $E_Z = g^* \mu_B B/2$, where g^* is the effective gyromagnetic factor and μ_B is the Bohr magneton. Let us assume that E_Z is much smaller than the Fermi energy yet sizeable in comparison to the mean level spacing inside the dot, Δ. The Zeeman splitting in the reservoirs amounts to a small shift in the wavelengths of the "up" and "down" electron states at the Fermi surface and nothing else. However, the effect in the quantum dot states can be much more pronounced. Since there are marked differences in the spatial distribution of eigenfunctions of states even if the are close in energy, changing the orbital content of states near the Fermi level will strongly affect the pumping current. Recall that the matrix elements of the scattering matrix fluctuate in energy for systems which have a chaotic dynamics in the classical limit. Therefore, by having $E_Z > \Delta$ we make the "up" and "down" components of the pumping current close to uncorrelated for a chaotic pump. If we define charge and spin pumping currents as[2]

$$I_c = I_\uparrow + I_\downarrow \tag{10}$$

and

$$I_s = I_\uparrow - I_\downarrow, \tag{11}$$

respectively, we see that while $I_s(B = 0) \equiv 0$ due to spin degeneracy, typically we have $I_s(B > B_c) \neq 0$, with B_c being a characteristic Zeeman field related to the pumping current correlation energy, E_c: $B_c = E_c/g^*\mu_B$. For weakly coupled quantum dots at very low temperatures E_c is equal to Δ. However, energy levels in open dots are broad resonances instead of sharp discrete levels. Moreover, lowest achievable temperatures with present technologies are comparable to the level spacing found in all but the smallest quantum dots. Thus, in the general case, $E_c = \max\{k_B T, \Delta, \hbar\gamma\}$, where γ is the electron escape rate (i.e., the inverse dwell time). This is scale is not too large: For a ballistic GaAs quantum dot[3] with a 1 μm in linear size and one open propagating channel per lead, one usually finds $\Delta = \pi\hbar\gamma \approx 10\,\mu$eV, leading to $B_c \approx 1$ T at temperatures below 100 mK.

In practice, one should avoid using a magnetic field perpendicular to the 2DEG underlying a lateral quantum dot. This is because even at fields of about 1 T there is already a significant reduction on the sensitivity of the wave functions to external perturbations (such as shape distortions) due to the formation of Landau states. This in turn reduces the dependence of the scattering matrix elements on parametric driving and, consequently, decreases the pumping current amplitude. Thus, a parallel magnetic field that only couples significantly to the electron spin and leaves the orbital motion unaltered is a more sensible choice for producing spin-polarized currents. The drawback is that this choice limits the spin polarization to only one direction.

[2] Here for convenience, we have adopted the same units for charge and spin currents.
[3] Electron densities are usually around 10^{11} cm^{-2} in high-quality GaAs wafers.

3.1 Pure Spin Currents

We have argued that phase coherence combined with wave function sensitivity to parametric changes make "up" and "down" spin components of an adiabatic pumping current nearly independent when even a moderate magnetic field is applied. This effect can be explored to produce dc spin transport with zero net charge transfer, the so-called pure spin current. The mechanism is illustrated in Fig. 3. The idea here is again based on the large sensitivity of confined quantum states to parametric changes when the underlying electronic motion is classically chaotic [29]. If a third tuning parameter, X_3 is provided besides the other two used to drive the system adiabatically, X_1 and X_2, such that $H = H(X_1, X_2, X_3)$, one can try to search for a realization of the Hamiltonian when "up" and "down" spin components of the pumping current have the same amplitude but opposite directions. This point is denoted in Fig. 3 by $X_{\rm ps}$. Notice that $I_s \neq 0$ while $I_c = 0$ at this point.

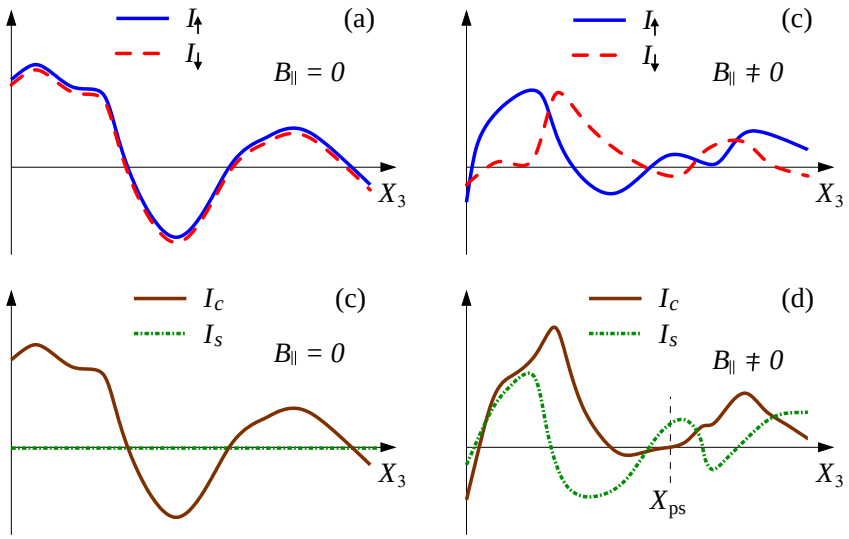

Fig. 3. Schematic plot of dc pumping currents as functions of a quantum dot tuning parameter X. The plots in (a) and (b) show the spin up and spin down components of the pumping current, $I_{\uparrow,\downarrow}$, the total charge I_c, and total spin currents I_s when no parallel magnetic field is applied, $B_{||} = 0$. Notice that in this case $I_s = 0$. In plots (c) and (d) $B_{||} \neq 0$, making $I_\uparrow \neq I_\downarrow$ and $I_s \neq 0$, in general. There are values of the tuning parameter, such as $X_{\rm ps}$, when a finite spin current occurs without net charge transport ($I_c = 0$)

3.2 Quantitative Analysis

When no spin-symmetric breaking field exists, both "up" and "down" spin components of the pumping current are identical. For an irregularly shaped quantum dot, as the amplitude of the external magnetic field is increased past the characteristic field B_c, the two spin components become uncorrelated. Since the ensemble averaged value of the dc pumping current is zero in the absence of bias, $\langle I_\uparrow \rangle = \langle I_\downarrow \rangle = 0$, we can write that

$$\mathrm{corr}_{\uparrow\downarrow}(B) \equiv \langle I_\uparrow \, I_\downarrow \rangle = \begin{cases} \langle I_\uparrow^2 \rangle, & B = 0, \\ 0, & B \gg B_c, \end{cases} \tag{12}$$

For intermediate values of the magnetic field, the correlation interpolates monotonically between the two limiting values.

The full spin polarization of the pumping current only occurs at those special configurations where $I_\uparrow = I_\downarrow$ exactly, regardless to how large the magnetic field is (provided it is nonzero). For all other configurations, the polarization will be smaller, random, and dependent on the magnetic field. In order to quantify the typical amplitude of the spin current in comparison to the charge current, we introduce the quantity $r_{\mathrm{pol}} = \sqrt{\langle I_s^2 \rangle / \langle I_c^2 \rangle}$. Both charge and spin currents can be written in terms of the correlation function $\mathrm{corr}_{\uparrow\downarrow(B)}$. It is then straightforward to show that

$$r_{\mathrm{pol}} = \sqrt{\frac{\mathrm{corr}_{\uparrow\downarrow}(0) - \mathrm{corr}_{\uparrow\downarrow}(B)}{\mathrm{corr}_{\uparrow\downarrow}(0) + \mathrm{corr}_{\uparrow\downarrow}(B)}} = \begin{cases} 0, & B = 0, \\ 1, & B \gg B_c. \end{cases} \tag{13}$$

This means that a substantial spin polarization may be achieved for sufficiently large magnetic fields, as we have anticipated using qualitative arguments in Sec. 3.1. Therefore, it is important to be able to quantify this effect, as well as the characteristic dependence of the spin current amplitude on temperature and on the number of propagating channel in the leads.

The non-trivial aspect of evaluating $\mathrm{corr}_{\uparrow\downarrow(B)}$ is that one needs to find a formulation where information about the energetics inside the dot can be incorporated. In other words, one has to be able to track down how wave functions and energy levels depend not only on the driving parameters but also on how scattering matrix elements corresponding to different spin orientations become progressively uncorrelated as the Zeeman splitting widens. Thus, a microscopic Hamiltonian formulation is unavoidable and the calculation cannot be performed within the static, random scattering matrix approach used by Brouwer [11].

Luckily, however, there are at least two ways to carry out the analytical calculation of $\mathrm{corr}_{\uparrow\downarrow(B)}$. Moreover, it is also possible to complement the analytical calculations with numerical simulations when the former become too involved. In our original work [25], we opted for suitably adapting a formulation developed by Vavilov and coworkers for the spinless *charge* pumping [30] variance. Their approach used the non-equilibrium Keldysh technique to

relate the instantaneous pumping current to the *real-time* scattering matrix of the dot using. Being very general and applicable beyond the adiabatic approximation, this formulation is rather sophisticated. However, as we show below, the extension to the non-zero Zeeman field case for the adiabatic regime is simple, can be worked out from the expressions found in Ref. [30], and yields the information about the correlation between the spin components of the pumping current that we are seeking.

Before going into the details of the calculation, it is important to highlight the assumptions used in the model. Vavilov and coworkers computed the pumping current assuming that: (i) the electron eigenstates of a non-interacting dot could be described the unitary ensemble of Gaussian random matrix and (ii) that the leads contained many propagating channels. These assumptions are well justified for the case of open dots with sufficiently complicated geometry, large contacts, and in the presence of a time-reversal symmetric breaking field. In practice, the latter condition can be enforced by letting the external magnetic field have a weak (tens of mT) perpendicular component.

Following Ref. [30], let us divide the total Hamiltonian of the total system into three parts,

$$H_{\text{total}} = H_{\text{dot}} + H_{\text{leads}} + H_{\text{dot}-\text{leads}}. \tag{14}$$

For the dot Hamiltonian we have

$$H_{\text{dot}} = \sum_{n,m=1}^{M} \sum_{\sigma=\pm 1} \left(\mathcal{H}_{n,m} + \delta_{n,m} \frac{\sigma E_Z}{2} \right) a_{n\sigma}^{\dagger} a_{m\sigma}, \tag{15}$$

where $a_{n\sigma}^{\dagger}, a_{n\sigma}$ are creation and annihilation electron operators defined over a single-particle basis of size M and $\{\mathcal{H}_{n,m}\}$ denote matrix elements of the orbital contribution to the electron energy on that basis. The spin-dependent, diagonal term accounts for the Zeeman energy. Notice that $\mathcal{H} = \mathcal{H}(t)$. For the leads Hamiltonian we have

$$H_{\text{leads}} = \sum_{\alpha=1}^{N} \sum_{k} \sum_{\sigma=\pm 1} \left[E(k) + \frac{\sigma E_Z}{2} \right] c_{\alpha k\sigma}^{\dagger} c_{\alpha k\sigma}, \tag{16}$$

where $c_{\alpha k\sigma}^{\dagger}, c_{\alpha k\sigma}$ are creation and annihilation electron operators in the leads, the index α runs over all $N = N_R + N_L$ propagating channels in the right and left leads, and $E_\alpha(k)$ is the electron energy dispersion relation in the channel α. Finally, for the dot-leads coupling Hamiltonian, we have

$$H_{\text{dot}-\text{leads}} = \sum_{\alpha,k,n,\sigma} \left(W_{n\alpha}\, c_{\alpha k\sigma}^{\dagger} a_{n\sigma} + \text{h.c.} \right), \tag{17}$$

where $W_{n\alpha}$ are coupling matrix elements related to the overlap between dot and lead single-particle wave functions at the contact regions. These matrix elements are assumed energy and spin independent.[4]

The dot single-particle Hamiltonian is separated into static and time-dependent or driving terms,

$$\mathcal{H}(t) = \mathcal{H}_0 + \lambda_1(t)\, X_1 + \lambda_2(t)\, X_2. \tag{18}$$

The static or unperturbed term $\mathcal{H}_0$ is taken to be a member of the Gaussian unitary ensemble with variance $\langle |[\mathcal{H}_0]_{n,m}|^2 \rangle = M\Delta^2/\pi^2$, where $M \gg 1$ is the matrix rank and Δ is the level space near the band center and where the Fermi level is located. The scalar functions $\lambda_1(t)$ and $\lambda_2(t)$ modulate the amplitude of the time-dependent perturbation. One usually chooses phase-locked, harmonic functions: $\lambda_1(t) = \cos(\omega t)$ and $\lambda_2(t) = \cos(\omega t + \varphi)$. It turns out that for sufficiently large dots, the diagonal parts of X_1 and X_2 are strongly suppressed and these matrices can be taken traceless. The strength of the perturbation is then fully characterized by only three numbers, namely $\mathrm{tr}(X_1^2)$, $\mathrm{tr}(X_2^2)$, and $\mathrm{tr}(X_1 X_2)$. These quantities can be related to the so-called "velocity" correlator [31], which measures how energy levels in the quantum dot respond to a linear, static perturbation of the form $\lambda_1 X_1 + \lambda_2 X_2$:

$$\frac{2\,\mathrm{tr}(X_i\, X_j)}{M^2} = \left\langle \frac{\partial \varepsilon_a}{\partial \lambda_i} \frac{\partial \varepsilon_a}{\partial \lambda_j} \right\rangle - \left\langle \frac{\partial \varepsilon_a}{\partial \lambda_i} \right\rangle \left\langle \frac{\partial \varepsilon_a}{\partial \lambda_j} \right\rangle, \tag{19}$$

where $\{\varepsilon_a(\lambda_1, \lambda_2)\}$ are the energy eigenvalues of the *isolated* quantum dot. This velocity correlator can be measured, thus providing information about the traces.

Two fundamental relations have to be used in this approach to write the pumping current in terms of the dot Hamiltonian. The first one is the standard connection between the scattering matrix and the scatterer (dot) Hamiltonian,

$$S_{\alpha\beta;\sigma}(t,t') = \delta_{\alpha,\beta}\, \delta(t-t') - 2\pi i \nu \sum_{n,m} W^*_{n\alpha}\, G^{(R)}_{nm;\sigma}(t,t')\, W_{m\beta}, \tag{20}$$

where ν is the density of states at the Fermi level and $G^{(R)}_{nm;\sigma}(t,t')$ is the retarded Green function of the *open* dot, satisfying the matrix equation

$$\left[i\hbar \frac{\partial}{\partial t} - \mathcal{H}(t) - \frac{\sigma E_Z}{2} + i\pi\nu W W^\dagger \right] G^{(R)}_\sigma(t,t') = \delta(t-t'). \tag{21}$$

The second relation is a connection between the total current flowing into one of the reservoirs[5] and the scattering matrix in real time,

[4] It is not too restrictive to assume that $W_{n\alpha}$ does not depend on the incoming or outgoing particle energy. The pumping current will still depend on the chemical potential in the leads through the Fermi distribution functions and the fact that $W_{n\alpha}$ depends on the dot state through n.

[5] Since charge is not accumulated during the pumping cycle, all current that flows from one of the reservoirs enters the other: $I^{\mathrm{left}} = -I^{\mathrm{right}}$

$$I_\sigma(t) = e\sum_\alpha \Lambda_{\alpha\alpha}\int\int dt_1\,dt_2\,\left[\sum_\beta S_{\alpha\beta;\sigma}(t,t_1)\tilde{f}_\beta(t_1-t_2)S^*_{\alpha\beta;\sigma}(t_2,t) - \tilde{f}_\alpha(+i0)\right], \tag{22}$$

where $\tilde{f}_\alpha(t)$ is the inverse Fourier transform of the electron Fermi-Dirac distribution function in the α channel,

$$\tilde{f}_\alpha(t) = \int_{-\infty}^{\infty}\frac{d\varepsilon}{2\pi}\,e^{i\varepsilon t/\hbar}\left[\frac{1}{e^{(\varepsilon-\mu_\alpha)/k_BT}+1}-\frac{1}{2}\right] = \frac{ik_BT\,e^{i\mu_\alpha t/\hbar}}{2\,\sinh(\pi k_BTt/\hbar)} \tag{23}$$

and Λ is the auxiliary matrix

$$\Lambda_{\alpha\beta} = \delta_{\alpha,\beta}\begin{cases} N_R/N, & \alpha\in\text{right lead},\\ -N_L/N, & \alpha\in\text{left lead}.\end{cases} \tag{24}$$

Equation (22) was derived in Ref. [30] under the standard assumption that the dispersion relation in the leads can be linearized: $E(k) = v_Fk$, where $v_F = 1/2\pi\nu$ is the Fermi velocity. Inserting (20) into (22) and assuming that no bias is present (such that we can drop the index α in both μ_α and f_α), it was found that

$$I_\sigma(t) = e\int\int dt_1\,dt_2\,\tilde{f}(t_1-t_2)\,\mathrm{tr}\left[R_\sigma(t,t_1,t_2)\right], \tag{25}$$

where we have introduced the matrix

$$R_\sigma(t,t_1,t_2) = 2\pi i\,\nu\,W^\dagger G^{(R)}_\sigma(t,t_1)\left[\mathcal{H}(t_1)-\mathcal{H}(t_2)\right]G^{(A)}_\sigma(t_2,t)W\Lambda. \tag{26}$$

At this point, there is an trick that can used when dealing with spin currents: Since the Zeeman energy splitting is uniformly present (inside and outside the quantum dot), it can be accounted for by a spin-dependent shift of the chemical potential. More specifically, if we make the substitution

$$\mu \to \mu + \frac{\sigma E_Z}{2}, \tag{27}$$

we can easily see that

$$\tilde{f}(t) \to e^{i\sigma E_Zt/2}\tilde{f}(t). \tag{28}$$

We can then drop the spin index from the Green functions in (26) and set the Zeeman energy to zero inside the dot. This allows us to reduce the ensemble-averaged correlator of dc spin components of the pumping current to

$$\begin{aligned}\mathrm{corr}_{\uparrow\downarrow}(B) &= \left(\frac{\omega}{2\pi}\right)^2\int_0^{2\pi/\omega}dt\int_0^{2\pi/\omega}dt'\,\langle I_\uparrow(t)\,I_\downarrow(t')\rangle\\ &= \left(\frac{e\,\omega}{2\pi}\right)^2\int\int\int\int dt_1\,dt_2\,dt_1'\,dt_2'\,e^{iE_Z(t_1-t_2+t_1'-t_2')/2}\\ &\quad\times\int_0^{2\pi/\omega}dt\int_0^{2\pi/\omega}dt'\,\left\langle\mathrm{tr}\left[R(t,t_1,t_2)\right]\mathrm{tr}\left[R(t',t_1',t_2')\right]\right\rangle.\end{aligned} \tag{29}$$

Thus, except for the Zeeman energy-dependent exponential factor in the integrand, the calculation amounts to same one performed by Vavilov and coworkers. They used a diagramatic technique based on random-matrix theory to evaluate the correlator $\left\langle \mathrm{tr}\,[R(t,t_1,t_2)]\,\mathrm{tr}\,[R(t',t_1',t_2')]\,\right\rangle$ in the limit of $N \gg 1$ and for perfectly transparent leads. The dimensionless parameter $1/N$ was used to regroup diagrams to leading order, yielding two-particle diffusion propagators similar to those used in the theory of disordered mesoscopic systems. The steps involved in their derivation are quite lengthy and we encourage the reader to check Ref. [30] for the details.

We can take their expression for $\left\langle \mathrm{tr}\,[R(t,t_1,t_2)]\,\mathrm{tr}\,[R(t',t_1',t_2')]\,\right\rangle$ [see (29) in Ref. [30]] and add the Zeeman-energy dependent exponential factor into the time integrations present in (29). In the adiabatic bilinear regime, the final expression for the spin current correlator becomes relatively compact:

$$\mathrm{corr}_{\uparrow\downarrow}(B) = \frac{e^2\omega^2 g\,\tau_\mathrm{d}\,\det(C)\,\sin^2\varphi}{2\pi^2}\int_0^\infty d\tau\, e^{-\tau/\tau_\mathrm{d}}\left(1+\frac{\tau}{\tau_\mathrm{d}}\right) \times\left[\frac{k_B T\tau/\hbar}{\sinh(\pi k_B T\tau/\hbar)}\right]^2\cos(\tau E_Z/2\hbar), \tag{30}$$

where $g = N_R N_L/N$ is the dot dimensionless conductance, $\tau_\mathrm{d} = 2\pi\hbar/N\Delta$ is the dwell time, and

$$C_{ij} = \frac{\pi}{M^2\Delta}\mathrm{tr}\,(X_i X_j)\,. \tag{31}$$

It is important to remark that (30) can also be derived using a semiclassical, trace formula representation of the scattering matrix. In that case, the validity of the semiclassical formulation is guaranteed by the large number of channels in the leads and the presumed chaotic electronic motion inside the dot. Details of the semiclassical calculation can be found in [21].

In Fig. 4 we show the resulting r_pol as a function of magnetic field for different temperatures and escape rates. Notice that thermal fluctuations have a relatively stronger effect on the polarization than the energy spreading due to the finite electron dwell time in the dot. The curves for the smallest values of N should be taken just as a qualitative indication of the dependence since (30) is only valid in the large-N limit.

4 Spin Current Detection

Once a spin-polarized current is generated through the mechanism presented in Sec. 3, the question that naturally arises is how to detect or measure the spin polarization. One could imagine using ferromagnetic leads to spin filter the current, like polarizers are used to filter out any component of a light beam. However, adding ferromagnetic leads is not yet a realistic option for lateral quantum dot setups. A more appropriate and readily available option is to use quantum point contacts (QPCs) where the width of the constriction can

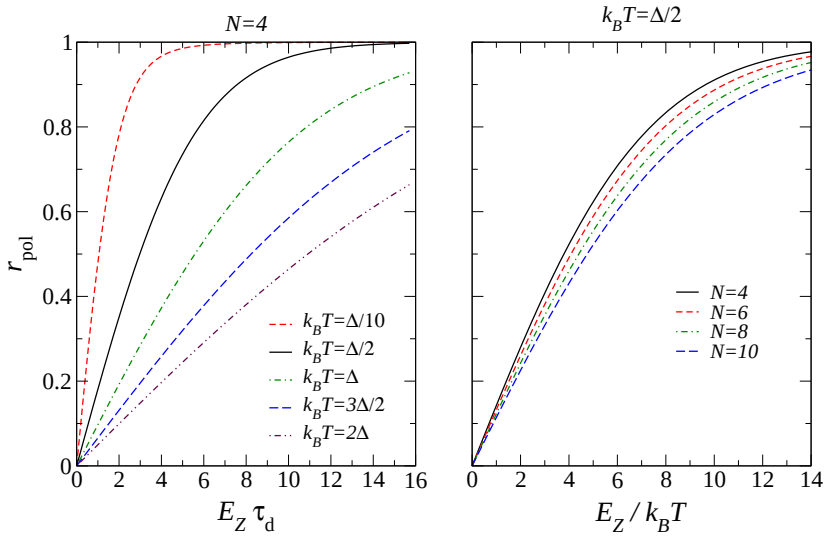

Fig. 4. The dependence of the relative spin polarization on the Zeeman splitting energy for (a) different temperatures and (b) for different number of propagating channels in the leads. Notice the different scales in the horizontal axes

be controlled by gate voltages [32]. A schematic view of such device connected to a spin pump is shown in Fig. 5.

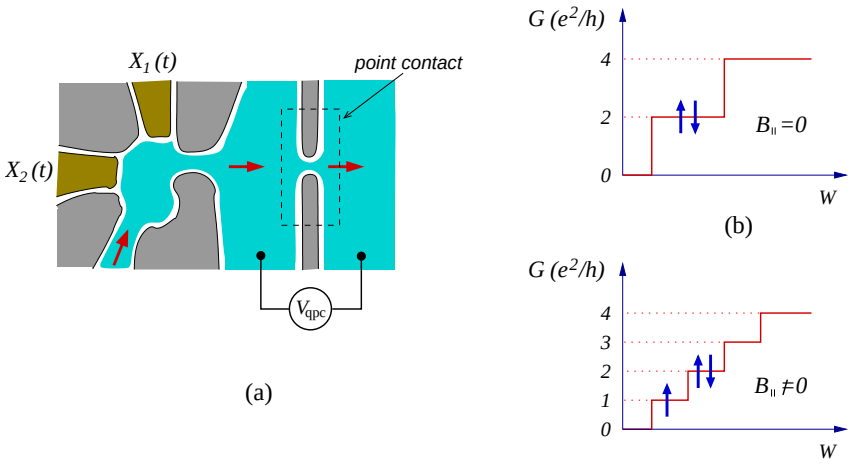

Fig. 5. (a) Schematic illustration of a quantum dot spin pump connected to a spin filtering point contact. The arrows indicate the direction of the current. (b) Linear conductance of the point contact as a function of the constriction width in the absence and in the presence of a parallel magnetic field

The detection works as follows. At sufficiently low temperatures and in the absence of a spin-splitting magnetic field, the conductance in the QPC is spin degenerate and presents steps at even values of the conductance quantum e^2/h [33]. When the spin-splitting field is turned on, the degeneracy is broken and intermediate steps appear at odd values of e^2/h. In this case, if one operates the QPC in the range where just one propagating channel is allowed, only the "up" spin component of the current will be transmitted and the "down" component will be filtered out. When the quantum pump is set to work at a configuration where $I_\uparrow = -I_\downarrow$ as to have a zero net flow of charge, the QPC will block $I_\downarrow$, resulting in $I_c \neq 0$ through the constriction a nonzero voltage drop across it ($V_{\rm qpc} \neq 0$). However, if the QPC conductance is brought to the second plateau at $2e^2/h$, both spin components are allowed to flow, making $I_c = 0$ and $V_{\rm qpc} = 0$ as well. Thus, by monitoring the voltage across the QPC the number of propagating channels goes from odd to even, it is possible to detect the spin current. When the pump works away from the pure spin configuration, $I_\uparrow$ and $I_\downarrow$ do not fully compensate each other and the charge current never drops to zero when the number of propagating channels in the QPC is even.

This scheme was implemented experimentally by Watson and coworkers [26]. In their setup a moderate perpendicular magnetic field was used to focus the current flow into the QPC (the cyclotron radius was considerably larger than the linear size of the effective well inside the dot, thus Landau level quantization was not sufficiently strong to impair parametric pumping.). Their results show clear evidence that spin polarization is achieved by parametrically driving the quantum dot in the presence of a parallel magnetic field. The spin current observed corresponded to tens of $\hbar$ per cycle at a frequency of 10 MHz. While this seems to confirm at least qualitatively our proposal, a complete test would also require collecting enough statistics to compare the statistics of the spin current to the theoretical predictions based on random matrix theory, as discussed in Sec. 4. This has yet to be done.

4.1 The Effect of Rectification

Giving the dominant presence of rectification effects in the earlier quantum pumping experiment by Switkes et al. [7], one could expect that a similar situation occurred in the experiment described in Ref. [26]. Indeed, this possibility cannot be discarded without a careful symmetry and statistical analysis of the pumping current. However, it turns out that the generation of spin-polarized currents is somewhat insensitive to the predominant mechanism, namely, even rectification due to spurious capacitive coupling between gate electrodes and the 2DEG would still lead to spin polarization. This can be easily understood if we recall that the conductance in the dot is susceptible to mesoscopic fluctuations during the pumping cycle. Therefore, dot conductance will vary in time as the pumping parameters run over a cycle. Now, if a certain spurious bias voltage $\delta V(t)$ occurs during the pumping cycle, an instantaneous rectification

current

$$\delta I_{\uparrow,\downarrow}(t) = G_{\uparrow,\downarrow}(t)\,\delta V(t) \tag{32}$$

will be added to the quantum pumping current. When the parallel magnetic field is present, $G_\uparrow(t) \neq G_\downarrow(t)$ since each spin component of the current is carried through the dot by a different composition of electronic states. As a result, after averaging over a full cycle, we will find $\overline{\delta I_\uparrow(t)} \neq \overline{\delta I_\downarrow(t)}$, leading to an additional contribution to the dc spin current.

A quantitative study of rectification effects requires a model circuit where the capacitive coupling between electrodes and leads is incorporated in a realistic way. Following the circuit model suggested by Brouwer [18], we have attempted to characterize the statistical properties of spin currents generated by rectification in Ref. [21]. The model circuit is shown in Fig. 6 for the case of a current setup. It is straightforward to find that [18, 21]

$$\delta I_{\uparrow,\downarrow}(t) = R_A G_{\uparrow,\downarrow}\left(\mathrm{C_{2L}}\frac{dX_1}{dt} + \mathrm{C_{1L}}\frac{dX_2}{dt}\right). \tag{33}$$

Using the semiclassical method, the correlation between "up" and "down" spin components of the rectified current was calculated under the same assumptions that led to (30). We have found that

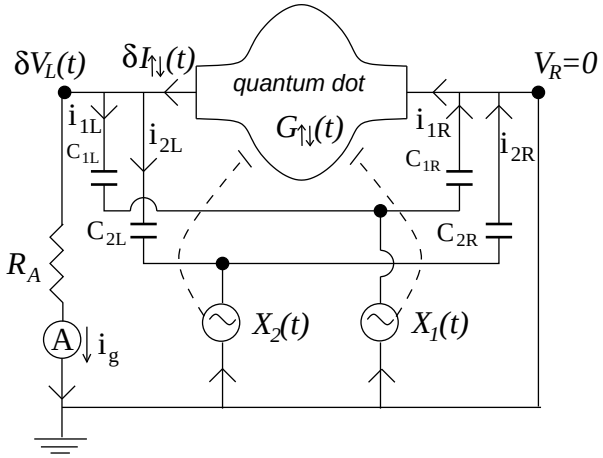

Fig. 6. Circuit model for the quantum pumping current measurement (current setup). The spurious capacitances between the electrode gates and the leads are denote by $\mathrm{C_{1R}}$, $\mathrm{C_{1L}}$, $\mathrm{C_{2R}}$, and $\mathrm{C_{2L}}$. R_A denotes the ampmeter internal resistance

$$\begin{aligned}\mathrm{corr}^{\mathrm{rect}}_{\uparrow\downarrow}(B) &= \langle \delta I_\uparrow\, \delta I_\downarrow \rangle \\ &= \mathcal{C}\int_0^\infty d\tau\, e^{-\tau/\tau_\mathrm{d}} \left[\frac{k_B T\tau/\hbar}{\sinh(\pi k_B T\tau/\hbar)}\right]^2 \cos(\tau E_Z/2\hbar),\end{aligned} \tag{34}$$

where $\mathcal{C}$ incorporates the characteristics of the dot and model circuit. Notice that this expression is very similar to (30). Indeed, using (34) instead of (30) to evaluate the polarization coefficient $r_{\rm pol}$ as a function of the magnetic field amplitude, we have found nearly identical curves to those shown in Fig. 4 [21]. Experimentally, it would be difficult to distinguish between pure quantum pumping and rectified spin currents on the basis of the magnetic field dependence of the correlations alone. Moreover, it turns out that even pure spin currents can be generated through rectification using the circuit model show in Fig 6. Thus, the most effective way to find out by how much the spin pumping current is contaminated by rectification remains the symmetry analysis described in Sec. 2.2.

4.2 Dephasing

Orbital decoherence will limit the amplitude of spin pumping currents in the same way it does for charge pumping. Since the quantum pumping is based on phase coherence within the dot it disappears altogether when the electron dephasing length is smaller than the dot linear size. That does not mean that currents will cease to be driven by parametrically cycling the dot, but just that the will be due to a classical pumping mechanism and rectification effects only.

However, the effect of decoherence is even more drastic in the case of spin pumping. That is because decoherence also washes out the spatial features of wave functions, causing states located at different energies to carry very similar pumping currents. This makes the Zeeman splitting less effective in uncorrelating "up" and "down" components of the current, decreasing the amplitude of the spin current. Notice that the same is true even if rectification is the main source of spin currents: As wave function "speckles" are smeared by dephasing, $G_\uparrow(t)$ and $G_\uparrow(t)$ becomes less distinguishable, reducing the amplitude of $\delta I_s = \overline{\delta I_\uparrow(t) - \delta I_\downarrow(t)}$ as well.

We have studied how decoherence impacts spin pumping in Ref. [21]. We followed the approach pioneered by Büttiker [35] where dephasing inside the dot is accounted for within the scattering matrix formalism by adding a third lead to the dot. The third lead carries no net current and has the sole purpose of steal or randomize the electron phase. The number of channels in the third lead, N_ϕ, is taken to be very large, but their coupling to the dot, p, is assumed very small. We can adjust the product pN_ϕ to produce a desired dephasing rate.

Our results show that for dots with a large number of propagating channels, setting pN_ϕ to yield realistic dephasing rates does impact the amplitude of the spin current fluctuations as much as thermal fluctuations. Fortunately, for the experimental conditions found in Ref. [26], dephasing plays a minor role in comparison to thermal smearing.

5 Summary and Future Directions

In this lecture we have argued that adiabatic pumping in open, lateral quantum dots can be used effectively to generate spin-polarized currents. The method is based on the phase coherence and the sensitivity of wave functions and energy levels inside the dot to changes in the shape of the confining potential. Realistic estimates based on random-matrix theory were presented and critical shortcomes such as spurious rectification and decoherence were addressed. Recently, the proposal passed its first experimental test. We hope that more groups will become interested in this subject.

During our presentation, we also left out some aspects which deserve further investigation. First, it is clear that the spin currents generated by this method can only be polarized parallel to the dot planar structure. In order to be achieve polarizations perpendicular to the plane or along any arbitrary direction one could explore the spin-orbit coupling intrinsic to asymmetric heterostructures (Rashba effect) and to semiconductors with no crystalline inversion symmetry (such as GaAs). A proposal along this direction already exists [24], but so far has not been implemented experimentally.

We have also not discussed spin relaxation as well as dissipation. There is strong evidence that spin-polarized currents travel considerable distances in GaAs 2DEG [36]. While pure dc spin currents lead to zero net charge or discharging, it is erroneous to believe that they are accompanied by no Joule dissipation. The electric power, when averaged over a full cycle, is nonzero. It is important to emphasize that dissipation increases substantially in the non-adiabatic regime.

A third aspect is how quantum pumping is affected by electron-electron interactions. It is well-known that the Coulomb interaction does not play an important role in transport properties of open quantum dots, namely, when channels in the leads are fully propagating [37]. The Coulomb interactions becomes important when the contacts are pinched so strongly that electrons have tunnel to enter or leave the quantum dot [12]. When the number of electrons in the dot is constrained to be an integer, charging effects take over and transport occurs only one electron at a time. In this case, the system resembles a classical turnstile pump and quantum interference plays essentially no role.

Although our proposed pump operates far from this regime, it would be very interesting to understand how one can interpolate between the fully open and the closed, Coulomb blockade regime. The difficulty lies in finding a formalism where both charging, many-body effects, phase coherence, and time-dependent driving can be put together. A few recent attempts along this direction have already been taken [38, 39]. Perhaps the most fascinating issue to be studied is the interplay between Kondo correlations and external driving. Such investigations might allows one to devise more efficient and controllable mechanisms to generate spin currents with quantum dots [40, 41, 42].

6 Acknowledgments

I am grateful to C. Chamon, C. Lewenkopf, C. Marcus, and M. Martínez-Mares for fruitful collaborations on this subject. The material presented here is based on published work we have co-authored. I also would like to thank P. Brouwer, B. Reulet, P. Sharma, and S. Watson for useful discussions.

References

1. M.A. Kastner: Rev. Mod. Phys. **64**, 849 (1992)
2. C.M. Marcus, A.J. Rimberg, R.M. Westervelt, P.F. Hopkins, A.C. Gossard: Phys. Rev. Lett. **69**, 506 (1992)
3. A.M. Chang, H.U. Baranger, L.N. Pfeiffer, K.W. West, T.Y. Chang: Phys. Rev. Lett. **76**, 1695 (1996)
4. L.P. Kouwenhoven *et al.*: In Nato ASI conference proceedings, Eds. L.P. Kouwenhoven, G. Schön, L.L. Sohn (Kluwer, Dordrecht 1997)
5. D. Goldhaber-Gordon, H. Shtrikman, D. Mahalu, D. Abusch-Magder, U. Meirav, M.A. Kastner: Nature **391**, 156 (1998)
6. S.M. Cronenwett, T.H. Oosterkamp, L.P. Kouwenhoven: Science **281**, 540 (1998)
7. M. Switkes, C.M. Marcus, K. Campman, and A.C. Gossard: Science **283**, 1905 (1999)
8. D.J. Thouless: Phys. Rev. B **27**, 6083 (1983)
9. B.L. Altshuler, L.I. Glazman: Science **283**, 1864 (1999)
10. B. Spivak, F. Zhou, M.T. Beal Monod: Phys. Rev. B **51**, 13226 (1995)
11. P.W. Brouwer: Phys. Rev. B **58**, R10135 (1998)
12. I.L. Aleiner, A.V. Andreev: Phys. Rev. Lett. **81**, 1286 (1998)
13. F. Zhou, B. Spivak, B.L. Altshuler: Phys. Rev. Lett. **82**, 608 (1999)
14. S.A. Wolf *et al.*: Science **294**, 1488 (2001)
15. I. Zutic, J. Fabian, S. Das Sarma: Rev. Mod. Phys. **76**, 323 (2004)
16. M. Büttiker, A. Prêtre, H. Thomas: Z. Phys. B **94**, 196 (1994)
17. J.E. Avrom, A. Elgart, G.M. Graf, L. Sadum: J. Stat. Phys. **116**, 425 (2004)
18. P.W. Brouwer: Phys. Rev. B **63**, 121303(R) (2001)
19. C.W.J. Beenakker: Rev. Mod. Phys. **69**, 731 (1997)
20. J.N.H.J. Cremers, P.W. Brouwer: Phys. Rev. B **65**, 115333 (2002)
21. M. Martínez-Mares, C.H. Lewenkopf, E.R. Mucciolo: Phys. Rev. B **69**, 085301 (2004)
22. I.L. Aleiner, B.L. Altshuler, A. Kamenev: Phys. Rev. B **62**, 10373 (2000)
23. M. Governale, F. Taddei, R. Fazio: Phys. Rev. B **68**, 155324 (2003)
24. P. Sharma, B.W. Brouwer: Phys. Rev. Lett. **91**, 166801 (2004)
25. E.R. Mucciolo, C. Chamon, C.M. Marcus: Phys. Rev. Lett. **89**, 146802 (2002)
26. S.K. Watson, R.M. Potok, C.M. Marcus, V. Umansky: Phys. Rev. Lett. **91**, 258301 (2003)
27. P. Sharma, C. Chamon: Phys. Rev. Lett. **87**, 096401 (2001)
28. R. Citro, N. Andrei, Q. Niu: Phys. Rev. B **68** 165312 (2003)
29. B.D. Simons, B.L. Altshuler: In *Mesoscopic Quantum Physics*, Eds. E. Akkermans, G. Montambaux, J.-L. Pichard, J. Zinn-Justin (Elsevier, 1994)

30. M.G. Vavilov, V. Ambegaokar, I.L. Aleiner: Phys. Rev. B **63**, 195313 (2001)
31. B.D. Simons, B.L. Altshuler: Phys. Rev. Lett. **70**, 4063 (1993)
32. J.A. Folk, R.M. Potok, C.M. Marcus, V. Umansky: Science **299**, 679 (2003)
33. B.J. van Wees *et al.*: Phys. Rev. Lett. **60**, 848 (1988)
34. M. Moskalets, M. Büttiker: Phys. Rev. B **64**, 201305(R) (2001)
35. M. Büttiker: Phys. Rev. B **33**, 3020 (1986)
36. J.M. Kikkawa, D.D. Awschalom: Phys. Rev. Lett. **80**, 4313 (1998)
37. P.W. Brouwer, I.L. Aleiner: Phys. Rev. Lett. **82**, 390 (1999). See also I. L. Aleiner, P.W. Brouwer, L.I. Glazman: Phys. Rep. **358**, 309 (2002)
38. J. Splettstoesser, M. Governale, J. König, R. Fazio: Phys. Rev. Lett. **95**, 246803 (2005)
39. E. Sela and Y. Oreg: preprint (cond-mat/0509457)
40. D. Feinberg, P. Simon: Appl. Phys. Lett. **85**, 4247 (2004)
41. M. Blaauboer, C.M.L. Fricot: Phys. Rev. B **71**, 041303 (2005)
42. E. Cota, R. Aguado, G. Platero: Phys. Rev. Lett. **94**, 107202 (2005)